Chinese Chemical Letters 35 (2024) 108943

Contents lists available at ScienceDirect

Chinese Chemical Letters

journal homepage: www.elsevier.com/locate/cclet

A novel and promising engineering application of carbon dots: Enhancing the chloride binding performance of cement

Wu-Jian Long, Yang Yu, Chuang He*

Guangdong Provincial Key Laboratory of Durability for Marine Civil Engineering, Key Lab of Coastal Urban Resilient Infrastructure, MOE, College of Civil and Transportation Engineering, Shenzhen University, Shenzhen 518060, China

ARTICLE INFO

Article history:
Received 17 July 2023
Revised 15 August 2023
Accepted 17 August 2023
Available online 19 August 2023

Keywords:
Carbon dots
Chloride binding
Cement
Chloride binding mechanism
Friedel's salt

ABSTRACT

Corrosion of reinforcement induced by chloride invasion is extensively considered as the dominating deterioration mechanism of reinforced concrete (RC) structures, leading to serious safety hazards and tremendous economic losses. However, it still lacks well dispersive and cost-efficient nanomaterials to improve the anti-chloride-corrosion ability of RC structures. Herein, specific carbon dots (CDs) with high dispersity and low cost are deliberately designed, successfully prepared by hydrothermal processing, and then firstly applied to immensely enhance chloride binding performance of cement, thereby contributing to suppressing the corrosion of reinforcement. Specifically, the tailored CDs are composed of the carbon core with highly crystalline sp^2 C structures and oxygen-containing groups connecting on the carbon core; The typical equilibrium test confirms that with respect to that of the blank cement paste, the chloride binding capacity of cement paste involving 0.2 wt% (by weight of cement) CDs is increased by 109% after 14-day exposure to 3 mol/L NaCl solution; according to comprehensive analyses of phase compositions, the chloride binding mechanism of CDs-modified cement is rationally attributed to the fact that the incorporation of CDs advances the formation of calcium silicate hydrate (C–S–H) gels and Friedel's salt (Fs), thus enormously enhancing the physically adsorbed and chemically bound chloride ions of cement pastes. This work not only firstly provides a novel high-dispersity and low-cost nanomaterial toward the durability enhancement of RC structures, but also broadens the application of CDs in the field of engineering, conducing to stimulating their industrialization development.

Reinforced concrete (RC) structures are extensively employed in major infrastructures such as bridges and buildings [1], thereby playing an irreplaceable role in the economic development. However, RC structures inevitably suffer from severe deterioration in complex coastal environment and deicing salts-applied locations, not only critically threatening the safety and reliability of related engineering, but also leading to enormous economic losses. For example, in 2014, the relevant economic losses exceeded 1 trillion Chinese Yuan in China, accounting for approximately 1.4% of Gross Domestic Product [2]. The primary factor for deterioration of RC structures is ascribed to the durability damage caused by the corrosion of reinforcement, while the chloride ingress is principally responsible for the corrosion of reinforcement [3–5]. When the concentration of invasive chloride on the reinforcement surface reaches the threshold value, the passivation layer of reinforcement will be subsequently destroyed, occasioning the initiation of electrochemical corrosion. Eventually, the RC structures will unavoidably crack owing to the corrosion-caused expansion of reinforcement.

To address the issue, multitudes of techniques involving corrosion inhibitor [6], anti-corrosion coating [7], cathodic protection [8] and chloride binding [9] have been developed to promote the anti-chloride-corrosion ability of concrete, thus mitigating the corrosion of reinforcement. Among them, corrosion inhibitor, anti-corrosion coating and cathodic protection can efficiently suppress the corrosion rate of reinforcement, but primarily highlight the protection strategy of prevention first. In other words, they fail to fundamentally reduce the concentration of chloride ions penetrating concrete. According to the corrosion mechanism of chloride ions [10], the intruded chloride ions cannot be consumed, but repeatedly destroy the passivation layer of reinforcement. Consequently, only by eliminating the free chloride ions inside concrete, can active anticorrosion of RC structures be achieved. Exhilaratingly, thoroughly different from above technologies, chloride binding technique is able to transform the free chloride ions into immobilized chloride ions, thereby reducing their concentration in concrete and enhancing the durability of RC structures. More

* Corresponding author.
E-mail address: hechuang@szu.edu.cn (C. He).

https://doi.org/10.1016/j.cclet.2023.108943
1001-8417/

specifically, by adding nanomaterials, mineral mixtures or chloride adsorption materials, the chloride binding approach can promote the formation of calcium silicate hydrate (C–S–H) gels or monosulfoaluminate hydrate (AFm) phases (reacting with free chloride ions to form Friedel's salt (Fs) or Kuzel's salt (Ks)), thus enormously enhancing the chloride physical adsorption or chemical binding of cement.

Benefiting from their advantages such as large specific surface area and less incorporation, nanomaterials demonstrate a more promising application prospect in chloride binding. Up to now, a range of nanomaterials including layered double hydroxides (LDHs), nano Al_2O_3, carbon nanotubes (CNTs) and graphene oxide (GO), have been applied to strengthen the chloride binding capacity of cement-based composites. For instance, Yang *et al.* found that regardless of the curing time of 7 or 28 d, the addition of 1.5 wt% CaFeAl-NO_3 LDHs in the simulated sea sand mortar sample made the free chloride content reduce by more than 32% than those of the blank sample, and attributed the eminent chloride binding performance of LDHs-incorporating cement to the formation of LDHs-Cl, Fs, and Ks [11]. Li *et al.* reported that after the incorporation of 7.5 wt% calcined LDHs (CLDHs) with the structural memory characteristic, the chloride binding capacity of mortar mixed with seawater and sea was greatly increased by 65%, assigned to effective chloride capture by recrystallization of CLDHs [12]. And CLDHs also accelerated the conversion of the ettringite (AFt) to the AFm phase, enhancing the chloride binding action of cement-based composites [13]. Besides LDHs and CLDHs, nano Al_2O_3 has also been applied to promote the chloride binding behavior of cementitious materials, since it stimulates the generation of more calcium silicoaluminate hydrate (C-A-S-H) gels (*i.e.*, the substitution of Si by Al in C–S–H gels) and Fs [9,14,15]. Yang *et al.* performed the equilibrium method to determine the positive effect of nano Al_2O_3 on the chloride binding, and revealed that bound chloride content of cement paste could be improved by 37.2% through introducing 5.0 wt% nano Al_2O_3 [9]. And nano Al_2O_3 could significantly boost the immobilized chloride ratio even at the long age of 180 d [14]. More recently, Li testified that CNTs could increase the chloride binding ability of concrete on account of their facilitation effect on the formation of more C–S–H gels [5], opening up a new avenue for the application of carbon-based nanomaterials. Inspired by this, Long *et al.* reported that the addition of 0.2 wt% GO made the chloride binding capacity of cement augment by 46% [16]. Despite tremendous progress, the research on nanomaterials employment in chloride binding technique is still in the infancy stage since the related literatures are less than 30. Hence, there are still a great number of barriers to be surmounted, among which poor dispersity and high cost are the most exigent problems. The former adversely affects not only the chloride binding ability [12], but also mechanical properties of cement-based materials [13]. The latter immensely hinders the actual application of nanomaterials. As a result, it is urgently necessary to exploit a high-dispersity and low-cost nanomaterial to enhance the chloride binding behavior of cement-based materials.

Carbon dots (CDs) act as a new type of zero-dimensional fluorescent carbon nanomaterial [17], serendipitously discovered in 2004 [18]. Due to their outstanding biocompatibility, attractive catalytic performance, prominent optical properties, tunable surface groups, high chemical stability, distinguished dispersity, diverse synthetic methods, easily available precursors, ultrasmall size and favorable environmental friendliness [19,20], CDs have been widely employed in biomedicine [21–23], catalysis [24–26], optoelectronic devices [27,28], sensing [29–31], lubrication [32,33], *etc*. However, the application of CDs in chloride binding technique has not been exploited yet. Based on the fact that CNTs and GO present the enhancement for the chloride binding ability of cement-based composites, CDs are expected to serve as a novel highly dispersed and cost-efficient nanomaterial to facilitate the chloride binding action of cement *via* rational design. In addition, the lack of mature and large-scale application scenarios gives rise to the much slower industrialization development of CDs compared with that of graphene discovered in the same year. If CDs are successfully used in the chloride binding field, it will not only contribute to improving the durability of RC structures, but also provide CDs with a promising engineering application. Therefore, more efforts should be made to design and prepare specific CDs for chloride binding technique.

In present work, the tailored CDs with the favorable crystalline carbon core and abundant oxygen-containing surface groups are elaborately designed according to both the existing chloride binding mechanism and the fact of CNTs and GO with chloride binding properties, and successfully fabricated *via* a hydrothermal method [34], then their chloride binding performance as the cement additive is comprehensively investigated by the typical equilibrium test [35] for the first time (Scheme 1). Remarkably, compared with other nanomaterials enhancing the chloride binding performance of cement, the tailored CDs possess the outstanding merits of low cost and high dispersity. After 14-day exposure to 3 mol/L NaCl solution, the chloride binding capacity of cement paste achieves a 109% improvement with the incorporation of 0.2 wt% (by weight of cement) CDs. Furthermore, the related chloride binding mechanism is rationally proposed based on exhaustive analyses of phase compositions by Fourier transform infrared spectroscopy (FTIR), X-ray diffraction (XRD), thermogravimetric analysis/differential thermogravimetric (TGA/DTG) and scanning electron microscope (SEM). These observations would be of fundamental importance, not only offering a novel high-dispersity and low-cost nanomaterial toward the durability enhancement of RC structures, but also opening up a promising way for the engineering application of CDs.

In general, a single CD consists of a carbon core and abundant surface groups. Based on their various structures, CDs can be divided into three categories: polymer dots (PDs), carbon nanodots (CNDs) and graphene quantum dots (GQDs) [36]. Specifically, PDs are regarded as cross-linked or aggregated polymers, possessing the amorphous carbon core; while CNDs are spherical morphology with lateral size roughly equal to their height, and own the carbon core with amorphous or graphite structures; with reference to GQDs, they hold single/several layers of graphene crystalline structures in their carbon core and connected functional groups on the edges, giving rise to the lateral dimension larger than their height. Based on the classification of CDs, the existing chloride binding

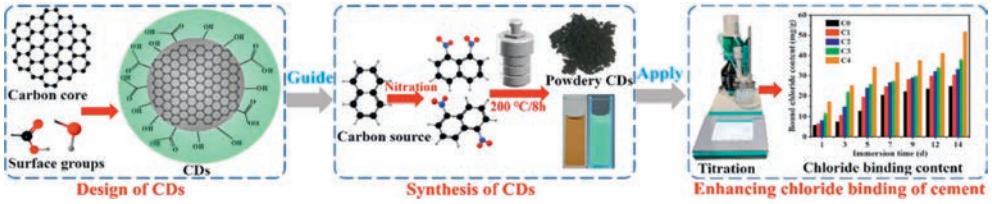

Scheme 1. Design, synthesis and engineering application of CDs.

mechanism and the fact of CNTs and GO with chloride binding properties, the carbon core and surface groups of CDs are deliberately designed in sequence: (1) The design of carbon core. In consideration of the fact that CNTs and GO are capable of promoting the chloride binding capacity of cement, the carbon core of CDs is designed to be the highly crystalline graphene structure, so that CDs can inherit the chloride binding ability of CNTs and GO. At the same time, the larger specific surface area of the carbon core is expected to endow CDs with more efficient chloride binding ability than CNTs and GO; (2) The design of surface groups. Surface groups not only play a crucial part in the chloride binding, but also directly affect the dispersity of nanomaterials in cement. As is widely acknowledged, owing to π-π stacking, van der Waals force and crosslinking with metal ions, carbon-based nanomaterials including CNTs and GO inevitably generate agglomeration in cement matrix [37]. Their poor dispersity is one of the most intractable problems [38], leading to negative effectiveness on cement hydration [39] and sharp increasing of cost [40]. To improve the dispersity of carbon core with crystalline graphene structure, it is necessary to carry out functional design for its surface. It has been substantiated that oxygen-containing groups such as –OH and –COOH not only enormously improve the dispersity of carbon-based nanomaterials [19], but also obviously accelerate the cement hydration [41], thereby tremendously boosting the content of C–S–H gels to enhance physically adsorbed chloride ions. More importantly, the carbon core of CDs can be easily modified by oxygen-containing groups using a facile one-step approach [34,42]. Thus, oxygen-containing groups are chosen as the surface groups of the designed CDs. To sum up, the designed CDs, expected to be suitable for the chloride binding technology, involve the carbon core with the highly crystalline graphene structure and oxygen-containing groups connecting on the carbon core (Fig. S1a in Supporting information). Their morphology and structure are similar to GQDs.

Up to now, a great number of routes have been developed to prepare CDs, including laser-ablation approach, chemical oxidation, microwave treatment, electrochemical synthesis, pyrolysis reaction and hydrothermal synthesis [19]. Among them, hydrothermal synthesis is considered as the most ideal way to effectively and simply synthesize CDs [43], since it effortlessly achieves controllable preparation of tailored CDs with a uniform size, specific surface groups and a tunable crystalline structure. Hence, hydrothermal treatment is selected to synthesize the designed CDs above. Meanwhile, it has been demonstrated that compared with bulk carbon materials such as CNTs, GO and coal, polycyclic aromatic hydrocarbon (PAH) molecules are more appropriate, more efficient and cheaper to serve as precursors for the preparation of crystalline GQDs (*i.e.*, the designed CDs) [34,44]. For instance, Wang *et al.* reported a gram-scale synthesis of single-crystalline and OH-functionalized GQDs with a high production yield of 63% by the molecular fusion of 1,3,6-trinitropyrene under mild hydrothermal conditions [44]. Recently, Yan *et al.* further corroborated that when the precursor was replaced by the simplest and cheapest PAH molecule of naphthalene, the production cost of CDs was decreased by several orders of magnitude, and their yield was increased to 71.3% [34]. As a consequence, in this work, the naphthalene is adopted as the precursor to prepare the designed CDs by mild hydrothermal treatment in NaOH aqueous solution at 200 °C for 8 h. The detailed growth process of CDs can be depicted as follows (Fig. S1b in Supporting information): Firstly, when naphthalene is treated by HNO_3, nitro groups as nucleophilic attack sites are introduced onto naphthalene; Subsequently, in NaOH aqueous solution under hydrothermal conditions, nitrated naphthalene molecules tend to fuse into the designed CDs through the elimination of hydrogen, condensation, graphitization and edge functionalization.

To certify the successful formation of the designed CDs, the morphology, structure, surface groups and optical properties of the as-obtained CDs are exhaustively characterized. The particle size distribution, morphology and topographic height of the as-prepared CDs are directly observed by TEM and AFM images, respectively. As shown in the TEM micrograph (Fig. 1a), CDs are quasi-spherical and well monodisperse without any aggregation, presenting a size distribution of 1.0–4.6 nm and an average size of *ca.* 2.63 nm by randomly counting more than 100 particles. The high-resolution TEM (HRTEM) image illustrates that the CDs possess favorable crystalline structures with well-resolved lattice fringes, and their lattice spacing of 0.21 nm well corresponds to the graphene (100) plane (Fig. 1b). The corresponding AFM image (Figs. 1c and d) reveals that the topographical height of the CDs falls in the range of 0.71–1.68 nm, indicating that the as-obtained CDs are GQDs. Other evidence supporting the observations drawn from TEM and AFM images is provided by XRD patterns and Raman spectra. XRD patterns (Fig. 1e) show an evident peak at approximately 27.2° in agreement with the graphite (002) plane [44], further unveiling graphitic crystallinity structures of the CDs. And owing to the small size of the CDs, their peak in XRD is broad [45]. As displayed in Fig. 1f, there are two obvious peaks at 1370 and 1574 cm^{-1} found in Raman spectra, assigned to the D band (disordered sp^3 defects) and G band (sp^2 carbon), respectively, and the intensity ratio of characteristic bands (I_D/I_G) is 0.87, further implying that the CDs have a high degree of crystallinity. Overall, the morphology and structure analyses above substantially evidence that the CDs with high crystallinity structures are successfully synthesized.

Surface groups and chemical compositions of the as-synthesized CDs are investigated by FTIR and XPS spectra. As depicted in FTIR spectra (Fig. 1g), the broad absorption band at 3444 cm^{-1} corresponds to the stretching vibration of –OH, strongly suggesting that the CDs are successfully decorated with −OH groups by means of nucleophilic attack by OH^- [34]. The characteristic adsorption band at 1388 cm^{-1} confirms the presence of C−OH groups, further implying the hydroxyl functionalization of the CDs [44]. Besides, a strong vibration at 1592 cm^{-1} is attributed to the C=C/C=O bonds [46,47]. The presence of C=C bonds proves the sp^2 C structure of the CDs, in accordance with the analyses from TEM, XRD and Raman. In addition, the absorption peaks at 1265 and 1070 cm^{-1} display the asymmetric and symmetric stretching vibration bands of C−O−C [48,49]. The diverse oxygen-containing groups connecting on the carbon core endow the CDs with excellent water solubility and dispersion stability, laying the foundation for their application in the cement matrix. The findings of FTIR spectra are testified by XPS measurement. In the full range XPS spectra, there are two strong peaks from C 1s (284 eV) and O 1s (532 eV) as well as a weak peak from impurity Na^+ (496 eV) (Fig. 1h). The high-resolution C 1s spectrum can be deconvolved into three peaks: C–C/C=C (284.1 eV), C–O (285.4 eV) and C=O (287.8 eV) (Fig. 1i). The C–C/C=C bonds account for a dominant content of 67.8%, further manifesting that the CDs are mainly composed of abundant sp^2 C structures. In the O 1s spectrum, three peaks are assigned to C=O (530.5 eV), C–O (532.1 eV) [50] and Na KLL (534.9 eV) (Fig. 1j). To sum up, the as-synthesized CDs are comprised of the carbon core with highly crystalline sp^2 C structures and oxygen-containing groups connecting on the carbon core, proving the successful preparation of the designed CDs.

The fluorescence is one of the main intrinsic properties of CDs [19]. The optical properties of the as-prepared CDs are measured by UV–vis and PL spectra. The UV–vis absorption spectrum (Fig. 1k) uncovers that the CDs have a weak shoulder peak at 298 nm, attributed to the $\pi-\pi^*$ transition of aromatic sp^2 domains of the carbon core. This result suggests that favorable crystalline structures of the CDs bring about the electron absorption state. As exhibited in PL spectra (Fig. 1L), the CDs aqueous solution shows yellow color when exposed to sunlight and emits the bright green

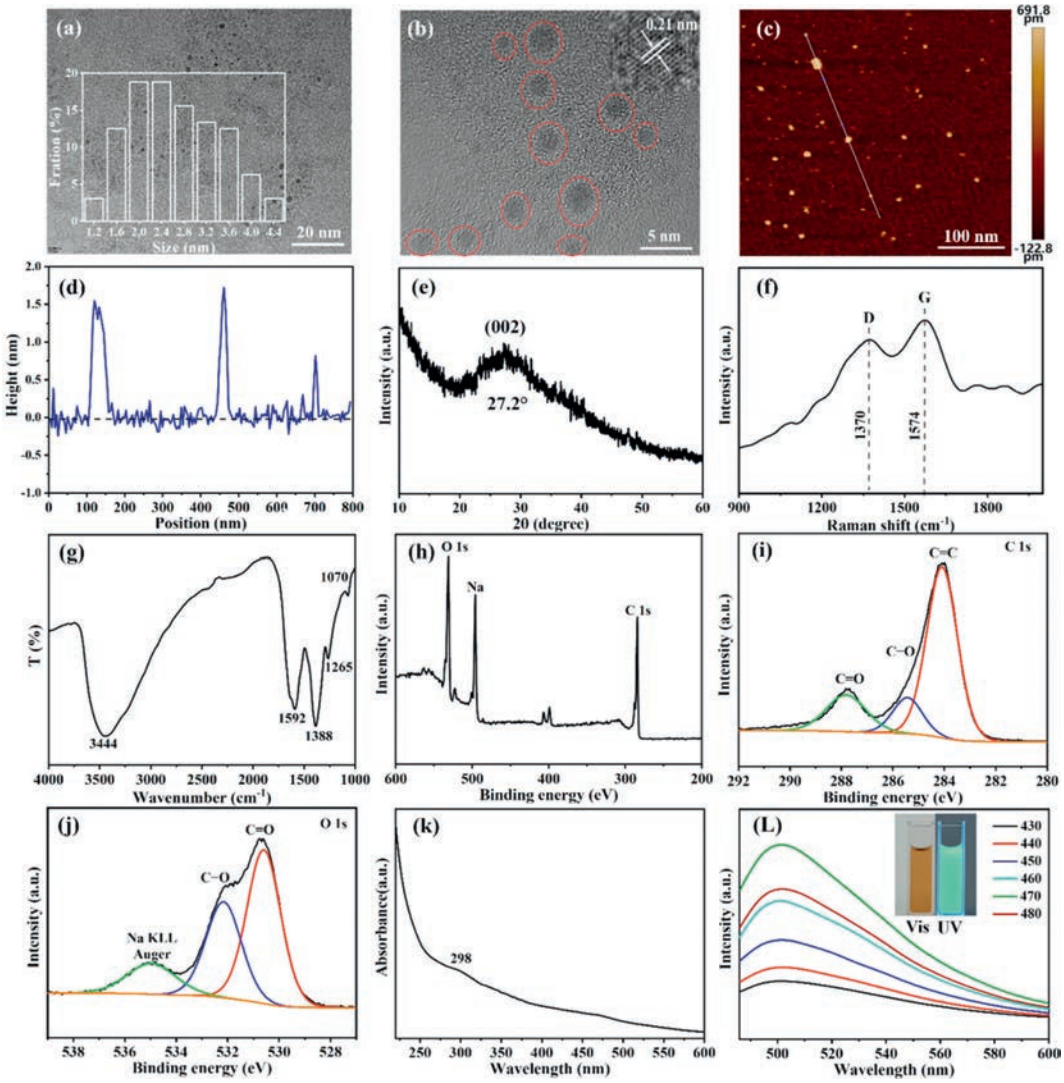

Fig. 1. The morphology and structure of the as-obtained CDs: (a) TEM (with a size distribution, inset) and (b) HRTEM images (with a lattice fringe of graphene (100) facet, inset); (c) AFM image and (d) the height profile along the white line in the AFM image; (e) XRD patterns; (f) Raman spectra. Surface groups, chemical compositions and optical properties of CDs: (g) FTIR spectra; (h) full range XPS spectra; (i) high-resolution XPS C1s and (j) O 1s spectra; (k) UV–vis and (L) PL spectra (with photographs taken under daylight and a 365 nm UV light, inset).

fluorescence excited by a 365 nm UV light. And the CDs with an excitation-independent PL action present the excitation/emission maximum at 470/501 nm. The above optical performance of the CDs offers a unique route to evaluate their dispersion stability in aqueous solution and simulated concrete pore solution (*i.e.*, saturation solution of $Ca(OH)_2$).

In a word, all the characterizations above reveal that the designed CDs are successfully synthesized by mild hydrothermal treatment using nitrated naphthalene molecules as the precursor, and their highly crystalline graphene structure and oxygen-containing groups are expected to improve the chloride binding ability of cement.

It is well-known that good dispersion stability of nanomaterials in cement-based materials is one of the significant prerequisites for the full use of their positive effects [51]. The dispersion stability of the as-synthesized CDs in aqueous solution and simulated concrete pore solution is validated on the basis of their optical behaviors. As displayed in Fig. 2, regardless of in aqueous solution or simulated concrete pore solution with 0.5 mg/mL CDs, there is no macroscopical precipitate after standing for two days at room temperature. When exposed to a 365 nm UV light, all the CDs-containing solutions emit bright green fluorescence, implying that the as-prepared CDs are well dispersive without agglomeration, since their agglomeration tends to make fluorescence weaken or vanish (namely self-quenching effect) [32]. Besides qualitative observations, UV–vis and maximum PL spectra of CDs before and after storage for 2 days are measured to quantitatively verify their distinguished long-term dispersion stability. According to the curves in Fig. 2, the intensities of UV–vis absorption peaks and emission maximum peaks from the CDs-incorporating aqueous solution and simulated concrete pore solution respectively remain almost unchanged. It should be noted that compared with those of CDs aqueous solution, PL spectra of CDs in alkali solution (*i.e.*, simulated concrete pore solution) undergo marked variations owing to the influence of deprotonation effect [52]. As a result, all the qualitative and quantitative observations suggest the excellent long-term dispersion stability of CDs in aqueous solution and simulated concrete pore solution, providing an essential precondition for CDs applications in cement-related fields.

To evaluate the influence of the CDs on the chloride binding properties of cement, chloride bound content (C_b) values of diverse cement pastes at different immersion time in 3 mol/L NaCl solution are recorded using the typical equilibrium test. As indicated in Fig. 3a, C_b values of all the samples evidently increase

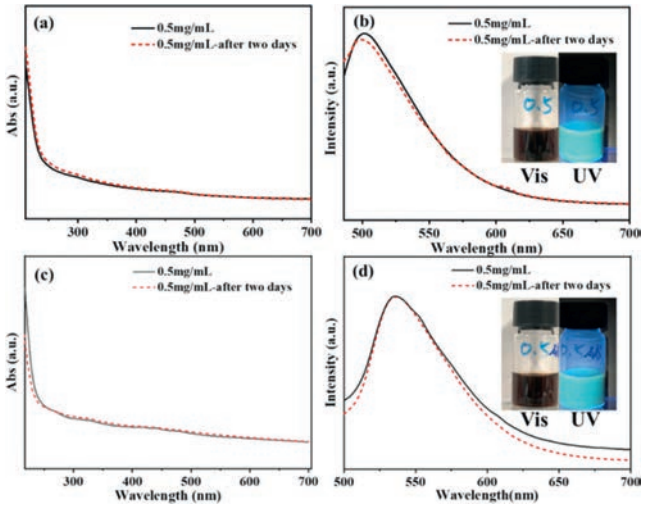

Fig. 2. (a) UV–vis spectra and (b) maximum PL spectra of CDs in aqueous solution (with photographs taken under daylight and a 365 nm UV light, inset) before and after two-day standing; (c) UV–vis spectra and (d) maximum PL spectra of CDs in simulated concrete pore solution (with photographs taken under daylight and a 365 nm UV light, inset) before and after two-day standing.

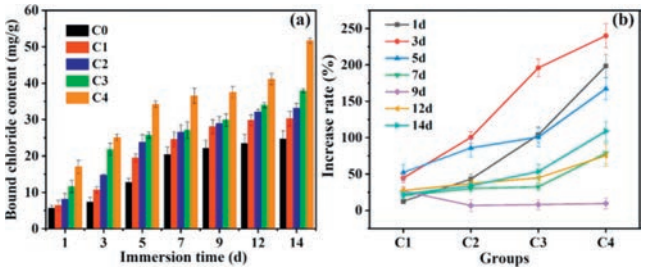

Fig. 3. (a) The C_b values of diverse cement pastes at different immersion time in NaCl solution; (b) the increase rates of C_b values from CDs-containing groups with respect to that of blank group at diverse immersion time.

with the extension of immersion time, and the incorporation of CDs can improve the C_b values regardless of the quantity of CDs addition or length of immersion time. The agglomeration of nanomaterials in cement-based composites inevitably diminishes their benefit. While regarding CDs, within the range of 0.2 wt% addition, the higher the addition, the higher C_b values. This implies the uniform dispersion of CDs in cement paste. Furthermore, with the extension of immersion time, the C_b values of all the groups gradually increase. These findings above indicate that the designed CDs are capable of sharply enhancing chloride binding abilities of cement pastes. In addition, almost all the CDs-containing groups reveal higher increase rates of C_b values at early immersion stage less than 7 d. More specifically, the C_b value of C4 group involving 0.2 wt% CDs is increased by 240% than that of blank group (C0 group) after 3-day exposure to NaCl solution, suggesting that the tailored CDs enable cement pastes to more rapidly immobilize free chloride ions. Besides, C4 group shows the highest C_b value of 51.66 mg/g at immersion time of 14 d, enhancing by 109% in comparison with that of C0 group (Fig. 3b). It is worth mentioning that in previous studies, the C_b value of cement paste could be promoted by only 46% with the incorporation of 0.2 wt% GO under similar testing conditions [16]. Hence, the designed CDs demonstrate a superior enhancement on the C_b value for cement paste, firmly testifying their more promising potential for practical applications in enhancing chloride binding performance of cement.

To investigate the chloride binding mechanism of CDs-modified cement pastes, FTIR spectra, XRD patterns, TGA/DTG curves and SEM images are adopted to analyze the phase compositions of various cement pastes before and after 14-day exposure to NaCl solution. As shown in normalized FTIR spectra (Fig. 4a), before immersion in NaCl solution, all the cement pastes with or without CDs present same characteristic peaks, testifying that all the groups contain identical hydration products, and CDs fail to alter the types of hydration products. Among them, the peaks at 1413 and 873 cm^{-1} are related to the CO_3^{2-} of $CaCO_3$ resulting from the carbonization reaction between CO_2 in the air and hydration products of $Ca(OH)_2$; while the peaks at 1113 and 957 cm^{-1} belong to S–O of AFt/AFm and Si–O of C–S–H gels, respectively [53]. After exposure to NaCl solution, there is a new peak at approximately 768 cm^{-1} in all the groups, ascribed to the Al–OH of Fs [54]. This observation exhibits that after exposure to NaCl solution, Fs is generated in all the cement pastes, thus achieving chemical binding for chloride ions. XRD patterns (Figs. 4b and c) further prove the result from FTIR spectra. Clearly, new peaks at 11°, 22° and 23° belonging to Fs appear in all the cement pastes after exposure to NaCl solution (Fig. 4c), further certifying that chemical binding for chloride ions induced by Fs is carried out. Furthermore, before exposure to NaCl solution, $Ca(OH)_2$ as the hydration product can be easily found in all the cement pastes, and $CaCO_3$ is inevitably formed owing to reaction between $Ca(OH)_2$ and CO_2 during the testing sample preparation. More specifically, $Ca(OH)_2$ in CDs-modified cement pastes shares more distinct peak at 18.1° than that of the blank cement paste, indicating that the CDs are supposed to accelerate hydration process of the cement [51] since CDs may offer nucleation sites [55]. At the same time, it can be inferred that CDs-modified cement pastes possess more C–S–H gels. As is well known, C–S–H gels are able to physically adsorb chloride ions by mutual attraction between charges. Hence, physical adsorption for chloride ions can be increased in CDs-modified cement pastes.

Since XRD test is not sensitive to minor phases, thus failing to quantificationally compare the content of Fs in different groups. TGA/DTG is adopted to get more detailed information. As shown in TGA curves (Fig. S3 in Supporting information), after 14-day immersion in NaCl solution, all the groups demonstrate curves with the similar downward trend. While CDs-containing groups hold more mass losses than blank group, meaning more hydration products formed in these groups. DTG curves (Fig. 4d) can identify different phases by mass losses in specific temperature intervals. Clearly, there are identical mass loss peaks in all the test specimens, further proving that the addition of CDs cannot change the classes of hydration products, which is consistent with results of FTIR and XRD. In detail, C–S–H gels as one of main hydration products continuously lose bound water between 40 °C and 600 °C with a central peak at roughly 100 °C [4] and the crystalline water of AFt is removed at 105–114 °C [56]. On account of the lower content of AFt, the mass loss peak ranging from 90 °C to 120 °C is predominated by C–S–H gels. For DTG curves, the stronger the mass loss peak, the more the corresponding phase. By comparison with blank group, CDs-modified groups have more C–S–H gels, and the addition of CDs is positively correlated with the content of C–S–H. This finding firmly supports the fact that CDs can promote the hydration process of cement pastes to generate more C–S–H gels. Thus, CDs significantly enhance the chloride physical adsorption action of cement pastes by more formation of C–S–H gels, in accordance with the deduction of XRD. Moreover, weight loss peaks in the regions of 120–230 °C and 240–350 °C are attributed to the decomposition of AFm and Fs respectively [57,58]. With reference to blank group, CDs-adding groups possess more AFm and Fs, of which C4 group exhibits the highest contents of AFm and Fs, reflecting that CDs are able to improve the transformation of AFt to AFm phase. And AFm can react with free chloride ions to form Fs under high chloride concentration environment. Correspondingly, more Fs is formed in CDs-modified specimens, thereby

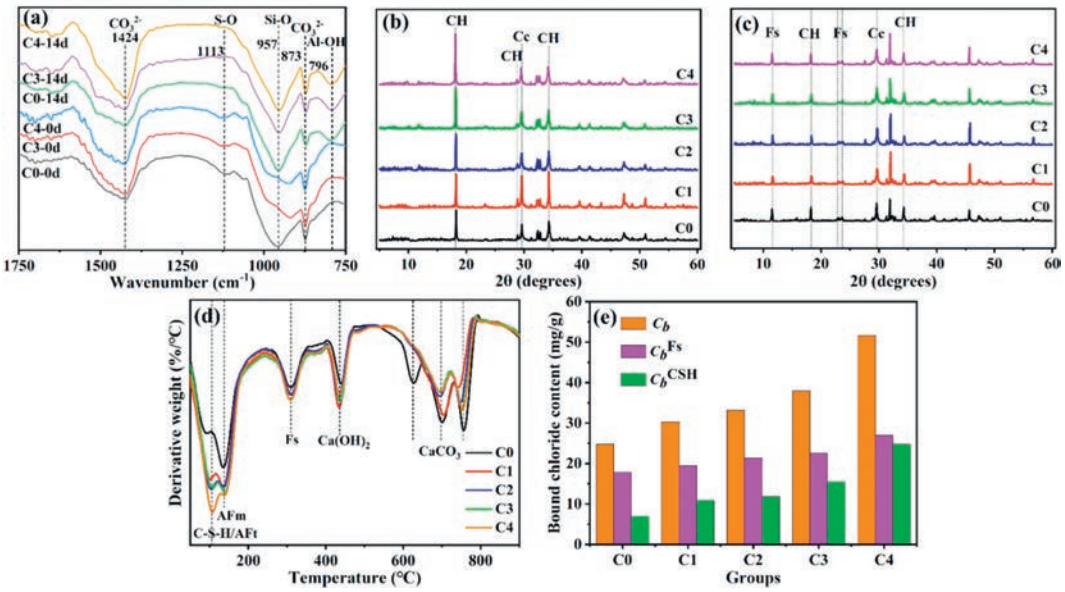

Fig. 4. (a) FTIR spectra and (b, c) XRD patterns (CH: $Ca(OH)_2$; Cc: $CaCO_3$) of different cement pastes before and after 14-day exposure to NaCl solution. (d) DTG of all the groups after 14-day exposure to NaCl solution. (e) Chloride distribution in Fs and C–S–H gels.

tremendously advancing the chloride chemical binding capacity of cement pastes. In addition, $Ca(OH)_2$ and $CaCO_3$ are decomposed at 400–470 °C and 600–800 °C, respectively.

Generally, the chloride binding of cement-based composites includes physical adsorption and chemical binding. The former is dominated by C–S–H gels and the latter is roughly equivalent to chlorine content in Fs. Apart from C–S–H gels and Fs, the chloride binding caused by other phases is considered to be negligible [16]. To confirm the chloride distribution in different phases, the chemically bound chloride (C_b^{Fs}) by Fs is firstly calculated according to Eq. S3 (Supporting information). And then the physically adsorbed chloride (C_b^{CSH}) caused by C-S-H gels is confirmed by Eq. 1.

$$C_b^{CSH} = C_b - C_b^{Fs} \quad (1)$$

The bound chloride distribution in Fs and C–S–H gels after 14-day exposure to 3 mol/L NaCl solution is illustrated in Fig. 4e. Unsurprisingly, the addition of CDs remarkably enhances values of C_b^{Fs} and C_b^{CSH}, and the higher the addition, the larger these values. As a result, C4 group simultaneously owns the highest C_b^{Fs} and C_b^{CSH} of 26.94 and 24.72 mg/g, increasing by 51% and 259% respectively than those of C0 group. These results are in agreement with the findings from TGA/DTG analyses, attributed to more formation of C–S–H gels and Fs in CDs-modified cement pastes. Additionally, chemical binding plays a principal role in chloride binding for CDs-adding cement pastes, in accordance with that of GO-incorporating cement pastes [16]. The obvious difference is that physical adsorption in CDs-adding cement pastes accounts for a larger proportion, and as the addition of CDs increases, the proportion of physical adsorption approaches 50%. This observation suggests that CDs with more oxygen-containing groups tend to boost more formation of C–S–H gels. It should be noted that CDs exhibit larger enhancement for C_b^{Fs} and C_b^{CSH} than GO under similar testing conditions [16], thus bearing greater potential to improve chloride binding capacities of cement-based materials.

The phase morphologies in cement pastes after 14-day exposure to NaCl solution are observed by SEM images (Fig. S4 in Supporting information). It has been demonstrated that $Ca(OH)_2$ crystals are normally hexagon sheet-shape. While Fs crystals also share the identical hexagonal flaky, but with a thinner thickness and a smaller size of 2–3 μm. And amorphous C–S–H gels are inclined to be irregularly fibrous or nano-granular. Regarding blank group without CDs (Fig. S4a), there are lots of thin and hexagonal-like Fs crystals with a haphazard distribution, and a few thick $Ca(OH)_2$ crystals with a larger size of *ca.* 4 μm randomly distributed among Fs crystals. After adding 0.05 wt% CDs, more Fs crystals are found in C2 group (Fig. S4b), evidencing that CDs can boost the formation of Fs, thereby improving the chloride chemical binding. Besides, possibly owing to coverage by Fs, fewer $Ca(OH)_2$ crystals are observed (Fig. S4b). Referring to C3 and C4 group (Figs. S4c and d), with the rising incorporation of CDs, the quantity of Fs crystals is further increased, which well corresponds to the results of TGA/DTG and chloride chemical binding. More importantly, the distribution of Fs crystals gradually becomes uniform, presenting a flower-like configuration. This finding implies that CDs are able to evenly dispersive in cement pastes, thus enhancing the formation of Fs crystals and improving their distribution from haphazard to uniformly flower-like construction. Additionally, in C3 and C4 groups (Figs. S4c and d), there are a great number of C–S–H gels adhering to Fs crystals, which conduces to boosting physical adsorption for chloride ions. All the above favorable impacts of CDs endow cement with enhanced chloride binding behaviors and potentially improved mechanical properties.

To summarize, the tailored CDs with multitudes of oxygen-containing groups can facilitate the transformation of AFt to AFm phase to increase the generation of Fs, and concurrently promote cement hydration to form more C–S–H gels. As a result, CDs play a positive part in both chloride chemical binding and physical adsorption of cement pastes. And within the range of 0.2 wt% addition, this positive effect is amplified by increasing CDs addition, with chloride physical adsorption benefiting the most. Furthermore, it needs to be emphasized that compared with previously reported GO [16], the designed CDs exhibit a more positive effect on cement pastes regardless of their chloride physical adsorption or chemical binding.

The chloride binding mechanism of CDs-modified cement is rationally proposed on the basis of the above-mentioned analyses (Fig. 5). That is the incorporation of CDs promotes the formation of C–S–H gels and Fs, thereby enormously boosting the physically adsorbed and chemically bound chloride ions of cement pastes. More specifically, it has been extensively demonstrated that nanomateri-

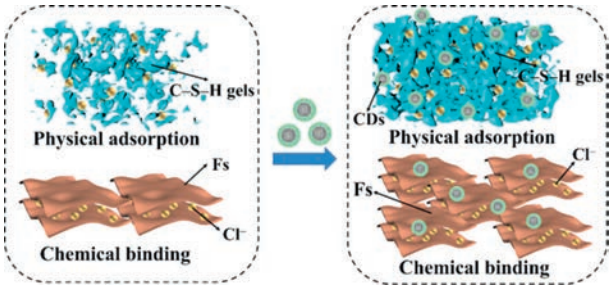

Fig. 5. Schematic illustration of chloride binding mechanism for cement pastes with and without CDs.

als can facilitate cement hydration by nucleation effect [51]. Generally, the nucleation effect for GO and CNTs is that the surface of GO/CNTs can adsorb calcium ions, thereby promoting the crystallization of hydrates and accelerating the hydration process [5,59]. Besides, GO/CNTs can also be tightly bonded to the C–S–H bundles by the bridge effect, presenting a good adhesive performance [5,60]. Benefiting from the synergetic contribution of bridge and nucleation effects, high-density and high-stiffness C–S–H gels also with a denser microstructure are easily generated. Regarding the tailored CDs with a small size of *ca.* 2.63 nm, they possess carbon core with highly crystalline graphene structures and numerous oxygen-containing groups connecting on the carbon core. Consequently, after incorporating CDs into cement, the carbon core of CDs functions as the nucleation site and bridge to facilitate more formation of high-quality C–S–H gels, working like GO and CNTs. According to the Electrical Double Layer theory, physical adsorption for chloride ions is principally assigned to the van der Waals attraction and electrostatic force between chloride ions and C–S–H gels [61]. Abundant high-density and high-stiffness C–S–H gels induced by CDs are conducive to significantly increasing physical adsorption for chloride ions. Moreover, numerous oxygen-containing groups greatly enhance the dispersity of CDs [19] regardless of in solution or cement paste, proved by optical characterization and SEM images. As is well known, the agglomeration of nanomaterials seriously compromises their practical benefit in cement [51]. Thus, excellent dispersity of CDs, together with their larger specific surface area, further exerts bridge and nucleation effects of carbon core, leading to the fact the designed CDs exhibit an outstanding improvement on the chloride physical absorption behavior of cement pastes. At the same time, oxygen-containing groups can also accelerate the cement hydration to generate more hydration products [41]. Apart from C–S–H gels, the designed CDs also promote the hydration of aluminum-containing minerals, and the transformation of AFt to AFm phase, verified by TGA/DTG. Thus, besides physical adsorption, chemical binding referring to the reaction between chloride ions and AFm to form Fs is also promoted by highly dispersed CDs. Ultimately, within the range of 0.2 wt% addition, the higher the CDs addition, the higher C_b values. The tailored CDs confer a more superior chloride binding ability on cement pastes than previously reported GO [16].

In summary, to effectively control the corrosion of reinforcement caused by chloride erosion, specifically designed CDs are successfully prepared by hydrothermal treatment, and then applied to enormously enhance the chloride binding performance of cement for the first time. Moreover, the chloride binding mechanism of CDs-modified cement is reasonably proposed. The main conclusions can be drawn as follows:

(1) Based on the classification of CDs, the existing chloride binding mechanism as well as the fact of CNTs and GO with chloride binding properties, CDs are deliberately designed to include carbon core with highly crystalline graphene structures and oxygen-containing groups connecting on the carbon core. The carbon core is expected to inherit the chloride binding ability of CNTs and GO, and oxygen-containing groups are advantageous in not only overcoming the agglomeration problem of nanomaterials, but also in increasing the chloride binding of cement.

(2) Adopting the naphthalene as the only precursor, the specifically designed CDs are effectively fabricated by mild hydrothermal treatment. The as-obtained low-cost CDs possess an average size of *ca.* 2.63 nm and a topographical height of 0.71–1.68 nm, and their surface are modified by oxygen-containing groups including −OH, C=O and C−O−C. More importantly, the as-obtained CDs demonstrate a long-term dispersion stability (for more than 2 days) in aqueous solution and simulated concrete pore solution. Thus, the as-prepared CDs surmount the toughest barriers of poor dispersity and high cost for applications of nanomaterials in cement-based materials.

(3) Using the typical equilibrium test, the chloride binding properties of various cement paste specimens with different CDs incorporation (0, 0.025, 0.05, 0.1 and 0.2 wt%) are measured. The results show that the higher the addition of CDs, the higher C_b values. And at the addition of 0.2 wt% CDs, the C_b value increases by 109% than that of blank group after 14-day exposure to 3 mol/L NaCl solution. The improvement in chloride binding performance of CDs-modified cement is much higher than that of GO-incorporating cement under similar testing conditions, substantiating more promising applications of CDs in chloride binding technique for cement.

(4) Based on extensive analyses of phase compositions through FTIR, XRD, TGA and SEM, the chloride binding mechanism of CDs-modified cement is rationally attributed to the fact that the incorporation of CDs greatly promotes the formation of Fs and C–S–H gels of cement pastes, thus enormously enhancing their chemical binding and physical adsorption for chloride ions.

These findings above not only afford a novel high-dispersity and low-cost nanomaterial toward the durability improvement of RC structures, but also broaden the application of CDs in the field of engineering, contributing to advancing the industrialization development of CDs.

Declaration of competing interest

The authors declare that they have no known competing financial interests or personal relationships that could have appeared to influence the work reported in this paper.

Acknowledgments

The research is financially supported by the National Natural Science Foundation of China-Youth Science Fund (No. 52208273) and the National Natural Science Foundations of China, NSFC-Shandong Joint Fund (No. U2006223). Furthermore, the authors thank Xinfang Cui from Shiyanjia Lab (www.shiyanjia.com) for AFM analyses. In addition, the authors appreciate Instrument Analysis Center of Shenzhen University for the assistance with TEM measurement.

Supplementary materials

Supplementary material associated with this article can be found, in the online version, at doi:10.1016/j.cclet.2023.108943.

References

[1] F. Zhang, C. Chen, R. Hou, et al., Corros. Sci. 153 (2019) 333–340.
[2] J. Hu, Y. Zhu, J. Hang, et al., Constr. Build. Mater. 267 (2021) 121011.

[3] W. Wilson, J.N. Gonthier, F. Georget, K.L. Scrivener, Cem. Concr. Res. 156 (2022) 106747.
[4] A. Babaahmadi, A. Machner, W. Kunther, et al., Cem. Concr. Res. 161 (2022) 106924.
[5] C. Li, J. Build. Eng. 41 (2021) 102419.
[6] F. Bolzoni, A. Brenna, M. Ormellese, Cem. Concr. Res. 154 (2022) 106719.
[7] F. Di Franco, A. Zaffora, B. Megna, M. Santamaria, Chem. Eng. J. 405 (2021) 126943.
[8] F. Wang, J. Xu, Y. Xu, L. Jiang, G. Ma, Constr. Build. Mater. 246 (2020) 118476.
[9] Z. Yang, Y. Gao, S. Mu, et al., Constr. Build. Mater. 195 (2019) 415–422.
[10] K. Subbiah, H.S. Lee, S. Mandal, T. Park, ACS Appl. Mater. Int. 13 (2021) 43676–43695.
[11] L. Yang, J. Xu, Y. Huang, et al., Constr. Build. Mater. 272 (2021) 122002.
[12] S. Li, Z. Jin, Y. Yu, Constr. Build. Mater. 293 (2021) 123493.
[13] Y. Xiang, G. Liang, H. Sun, H. Li, D. He, Constr. Build. Mater. 320 (2022) 126325.
[14] X. Liu, B. Ma, H. Tan, et al., Constr. Build. Mater. 220 (2019) 43–52.
[15] Z. Yang, S. Sui, L. Wang, et al., Constr. Build. Mater. 232 (2020) 117219.
[16] W.J. Long, X. Zhang, G.L. Feng, et al., Cem. Concr. Compos. 132 (2022) 104603.
[17] X. Yang, X. Li, B. Wang, et al., Chin. Chem. Lett. 33 (2022) 613–625.
[18] X. Xu, R. Ray, Y. Gu, et al., J. Am. Chem. Soc. 126 (2004) 12736–12737.
[19] C. He, P. Xu, X. Zhang, W. Long, Carbon 186 (2022) 91–127.
[20] C. He, S. E, H. Yan, X. Li, Chin. Chem. Lett. 32 (2021) 2693–2714.
[21] S. E, C. He, J.H. Wang, Q. Mao, X. Chen, ACS Nano 15 (2021) 14465–14474.
[22] J. Hu, Y. Guo, X. Geng, et al., Chem. Eng. J. 446 (2022) 136928.
[23] Y. Zhang, H. Xia, M. Yang, et al., Chin. Chem. Lett. 34 (2023) 108197.
[24] J. Zhuang, S. Ren, B. Zhu, et al., Chem. Eng. J. 446 (2022) 136873.
[25] X. Wang, M. Wang, G. Liu, et al., Nano Energy 86 (2021) 106122.
[26] Y. Zhou, X. Lu, Y.C. Chang, et al., Chin. Chem. Lett. 34 (2023) 107888.
[27] B. Wang, H. Song, Z. Tang, B. Yang, S. Lu, Nano Res. 15 (2021) 942–949.
[28] C. He, H. Yan, X. Li, X. Wang, Mater. Res. Express 6 (2019) 065609.
[29] Y. Xu, Y. Yang, S. Lin, L. Xiao, Anal. Chem. 92 (2020) 15632–15638.
[30] G. Zou, S. Chen, N. Liu, Y. Yu, Chin. Chem. Lett. 33 (2022) 778–782.
[31] F. Shan, L. Fu, X. Chen, et al., Chin. Chem. Lett. 33 (2022) 2942–2948.
[32] C. He, H. Yan, X. Li, X. Wang, Green Chem. 21 (2019) 2279–2285.
[33] Z. Mou, Q. Yang, J. Peng, et al., J. Colloid Interface Sci. 623 (2022) 762–774.
[34] Y. Yan, D. Zhai, Y. Liu, et al., ACS Nano 14 (2020) 1185–1195.
[35] L.P. Tang, L.O. Nilsson, Cem. Concr. Res. 23 (1993) 247–253.
[36] S.J. Zhu, Y.B. Song, X.H. Zhao, et al., Nano Res. 8 (2015) 355–381.
[37] S. Ding, Y. Xiang, Y.Q. Ni, et al., Nano Today 43 (2022) 101438.
[38] Y. Sargam, K. Wang, A. Tsyrenova, F. Liu, S. Jiang, Cem. Concr. Res. 144 (2021) 106417.
[39] J.A. Oh, M. Aakyiir, Y. Liu, et al., Cem. Concr. Compos. 125 (2022) 104321.
[40] P. Feng, H. Chang, X. Liu, et al., Mater. Des. 186 (2020) 108320.
[41] G. Jing, J. Wu, T. Lei, et al., Constr. Build. Mater. 248 (2020) 118699.
[42] S. E, Q.X. Mao, X.L. Yuan, et al., Nanoscale 10 (2018) 12788–12796.
[43] W.J. Long, X.Q. Li, Y. Yu, C. He, J. Mol. Liq. 360 (2022) 119522.
[44] L. Wang, Y. Wang, T. Xu, et al., Nat. Commun. 5 (2014) 5357.
[45] L.B. Tang, R.B. Ji, X.K. Cao, et al., ACS Nano 6 (2012) 5102–5110.
[46] W. Li, D. Yoon, J. Hwang, W. Chang, J. Kim, J. Power Sources 293 (2015) 1024–1031.
[47] M. Xu, G. He, Z. Li, et al., Nanoscale 6 (2014) 10307–10315.
[48] L.H. Mao, W.Q. Tang, Z.Y. Deng, et al., Ind. Eng. Chem. Res. 53 (2014) 6417–6425.
[49] R. Fu, H. Song, X. Liu, et al., Chin. J. Chem. 41 (2023) 1007–1014.
[50] B. Wang, Z. Wei, L. Sui, et al., Light Sci. Appl. 11 (2022) 172.
[51] W.J. Long, P. Xu, Y. Yu, F. Xing, C. He, Cem. Concr. Compos. 134 (2022) 104782.
[52] W.J. Long, X.Q. Li, S.Y. Zheng, et al., Carbon 218 (2024) 118708.
[53] F. Qu, W. Li, K. Wang, V.W.Y. Tam, S. Zhang, Constr. Build. Mater. 310 (2021) 125229.
[54] X. Wang, W. Ni, R. Jin, B. Liu, Constr. Build. Mater. 220 (2019) 119–127.
[55] H. Qu, S. Qian, X. Liu, et al., J. Build. Eng. 52 (2022) 104523.
[56] P. Hemstad, A. Machner, K. De Weerdt, Cem. Concr. Res. 130 (2020) 105976.
[57] Z. Shi, M.R. Geiker, K. De Weerdt, et al., Cem. Concr. Res. 95 (2017) 205–216.
[58] S. Krishnan, S. Bishnoi, Cem. Concr. Res. 108 (2018) 116–128.
[59] S. Meng, X. Ouyang, J. Fu, Y. Niu, Y. Ma, Nanotechnol. Rev. 10 (2021) 768–778.
[60] D. Hou, Z. Lu, X. Li, H. Ma, Z. Li, Carbon 115 (2017) 188–208.
[61] Y. Elakneswaran, T. Nawa, K. Kurumisawa, Cem. Concr. Res. 39 (2009) 340–344.